Catalysis Science & Technology

PAPER

View Article Online
View Journal | View Issue

Cite this: *Catal. Sci. Technol.*, 2014, 4, 1931

Photocatalytic reactions under irradiation of visible light over gold nanoparticles supported on titanium(IV) oxide powder prepared by using a multi-step photodeposition method†

Atsuhiro Tanaka, Satoshi Sakaguchi, Keiji Hashimoto and Hiroshi Kominami*

Received 13th January 2014,
Accepted 11th February 2014

DOI: 10.1039/c4cy00042k

www.rsc.org/catalysis

Titanium(IV) oxide (TiO_2) having both smaller and larger gold (Au) particles was successfully prepared by a multi-step (MS) photodeposition method. When 0.25 wt% Au loading per photodeposition was repeated four times, smaller and larger Au particles having average diameters of 1.4 and 13 nm, respectively, were fixed on TiO_2, and the Au/TiO_2 sample exhibited strong photoabsorption around 550 nm due to surface plasmon resonance (SPR) of the larger Au particles. Various Au/TiO_2 samples were prepared by changing the Au loading per photodeposition and the number of photodepositions. Effects of the conditions in MS photodeposition and sample calcination on Au particle distribution and photoabsorption properties were investigated. These samples were used for hydrogen (H_2) formation from 2-propanol and mineralization of acetic acid in aqueous suspensions under irradiation of visible light. In the case of H_2 formation under deaerated conditions, the reaction rate of Au/TiO_2 having both larger and smaller particles was 4 times higher than that of the Au/TiO_2 sample without smaller Au particles, indicating that smaller Au particles acted effectively as a co-catalyst, that is, as reduction sites for H_2 evolution. On the other hand, in the case of mineralization of acetic acid under aerated conditions, carbon dioxide formation rates were independent of the presence of smaller Au particles, indicating that the smaller Au particles had little effect on the mineralization of acetic acid. To extend the possibility of Au/TiO_2 for H_2 formation under irradiation of visible light, H_2 formation from ammonia (NH_3) as biomass waste was examined under deaerated conditions; NH_3 was decomposed to H_2 and nitrogen with a stoichiometric ratio of 3 : 1.

Introduction

Various reactions including oxidation of organic compounds,[1] reduction of aromatic compounds[2] and hydrogen (H_2) production[3] by semiconductor photocatalysts such as titanium(IV) oxide (TiO_2) have attracted much attention. In the case of H_2 production, TiO_2 represents a promising technology to use renewable resources for clean and environmentally friendly energy production. TiO_2 is a wide band gap photocatalyst (band gap = 3.2 eV) that can induce evolution of H_2 from various compounds under ultraviolet (UV) light irradiation.[1–3] However, UV light accounts for only about 5% of the total solar energy, while visible light accounts for about 50% of the total solar energy. Therefore, the development of photocatalysts using visible light is an important topic from a practical point of view.

Department of Applied Chemistry, Faculty of Science and Engineering, Kinki University, Kowakae, Higashiosaka, Osaka 577-8502, Japan.
E-mail: hiro@apch.kindai.ac.jp

† Electronic supplementary information (ESI) available: Fig. S1 and S2. See DOI: 10.1039/c4cy00042k

Modification of TiO_2 photocatalysts has often been used to extend their absorption wavelength from the UV region to the visible region. To the best of our knowledge, these photocatalysts can be roughly classified into two types. The first type is TiO_2 doped with nitrogen[4] and sulfur[5] as bulk modifiers. The energy levels of nitrogen and sulfur are inserted in the forbidden band of TiO_2, resulting in the response to visible light. The second type is semiconductors modified with metal ions such as copper ions (Cu^{2+}) utilizing interface charge transfer (IFCT)[6] and TiO_2 samples modified with inorganic sensitizers such as platinum(IV) and rhodium(III) chlorides.[7]

Unique optical properties of gold (Au) nanoparticles have been applied in many fields including biochemistry, sensing science, and catalysis.[8] Nanoparticles of Au show strong photoabsorption of visible light at around *ca.* 550 nm due to surface plasmon resonance (SPR). SPR of Au nanoparticles has been applied to visible light-responding photocatalysts.[9–11] These photocatalysts have been widely used for SPR-induced photoabsorption in chemical reactions, *i.e.*, oxidation of organic substrates,[10d,e,11a–c,g] selective oxidation of aromatic alcohols to

carbonyl compounds,[10c,11d,f] H_2 formation from alcohols,[10f,g,11e,h] dioxygen (O_2) formation from water in the presence of hexavalent chromium as an electron scavenger[11k] and selective reduction of organic compounds.[10h,11j] In our previous communication,[11e] we described a multi-step (MS) photodeposition method for the preparation of Au/TiO_2 samples, in which photodeposition of Au was divided into several steps; for example, photodeposition of 0.25 wt% Au was repeated four times to obtain a 1.00 wt% Au/TiO_2 sample. We reported that Au/TiO_2 samples prepared by the MS photodeposition method (MS-Au/TiO_2) exhibited stronger photoabsorption at around 550 nm due to SPR and higher levels of activity for H_2 production under irradiation of visible light. Since MS-Au/TiO_2 samples exhibited a unique bimodal distribution of Au particles, we suggested that functions of Au/TiO_2 could be shared by Au particles with different sizes, *i.e.*, small Au particles as co-catalysts for H_2 formation and large Au particles for photoabsorption and oxidation. Here, we report 1) precise control of Au particle distribution by the MS photodeposition method, 2) factors controlling properties and the photocatalytic activity of Au/TiO_2 samples and 3) the function of Au as a co-catalyst.

2. Experimental

2.1 Synthesis of nanocrystalline TiO_2

Nanocrystalline TiO_2 powder was prepared using the HyCOM (hydrothermal crystallization in organic medium) method at 573 K.[12] Titanium(IV) butoxide and toluene were used as the starting material and solvent, respectively. The product was calcined at 723 K for 1 h in a box furnace. The crystallinity of HyCOM-TiO_2 samples was improved by calcination, and the samples still had a large specific surface area of 97 $m^2\ g^{-1}$ even after calcination at 723 K. Hereafter, a calcined HyCOM-TiO_2 sample is designated as TiO_2(calcination temperature); for example, a sample calcined at 723 K is shown as TiO_2(723).

2.2 Preparation of Au/TiO_2

Loading of Au on TiO_2 was performed by a photodeposition method. Bare TiO_2 powder (198 mg) was suspended in 10 cm^3 of an aqueous solution of methanol (50 vol%) in a test tube and the test tube was sealed with a rubber septum under argon (Ar). An aqueous solution of tetrachloroauric acid ($HAuCl_4$) was injected into the sealed test tube and then photoirradiated at $\lambda > 300$ nm by a 400 W high-pressure mercury arc (Eiko-sha, Osaka, Japan) under Ar with magnetic stirring in a water bath continuously kept at 298 K. The Au source was reduced by photogenerated electrons in the conduction band of TiO_2, and the Au metal was deposited on TiO_2 particles, resulting in the formation of Au/TiO_2. Analysis of the liquid phase after each photodeposition revealed that the Au source had been almost completely (>99.9%) deposited as Au on the TiO_2 particles. The resultant powder was washed repeatedly with distilled water and then dried at 310 K overnight under air. In the MS photodeposition method, photodeposition of Au was repeated several times to obtain an Au/TiO_2 sample having a desired Au content. Hereafter, a sample prepared by the MS photodeposition method is designated as Au($X \times Y$)/TiO_2, where X and Y mean the amount of Au in wt% per photodeposition and the number of photodepositions, respectively. For example, Au(0.25×4)/TiO_2 was prepared by repeating 0.25 wt% photodeposition four times. In this study, the total amount of Au was fixed at 1.0 wt% ($X \times Y = 1.0$).

2.3 Characterization

Diffuse reflectance spectra of Au/TiO_2 samples were obtained using a UV-visible spectrometer (UV-2400, Shimadzu, Kyoto) equipped with a diffuse reflectance measurement unit (ISR-2000, Shimadzu). The morphology of Au/TiO_2 samples was observed under a JEOL JEM-3010 transmission electron microscope (TEM) operated at 300 kV in the Joint Research Center of Kinki University. The spectrum and light intensity of the Xe lamp (filtered) were determined using a spectroradiometer USR-45D (Ushio, Tokyo).

2.4 Photocatalytic activity tests

2.4.1 H_2 formation from 2-propanol in aqueous suspensions of Au/TiO_2 under irradiation of visible light. Dried photocatalyst powder (50 mg) was suspended in 50 vol% 2-propanol–water solution (5 cm^3), bubbled with Ar, and sealed with a rubber septum. The suspension was irradiated with visible light from a 500 W xenon (Xe) lamp (Ushio, Tokyo) filtered with a Y-48 filter (AGC Techno Glass) (450–600 nm; 83 mW cm^{-2}) with magnetic stirring in a water bath continuously kept at 298 K. The amount of H_2 in the gas phase was measured using a Shimadzu GC-8A gas chromatograph equipped with an MS-5A column. The amount of acetone in the liquid phase was determined using a Shimadzu GC-14A gas chromatograph equipped with a fused silica capillary column (HiCap-CBP20, 25 m, 0.22 mm). Toluene was used as the internal standard sample. The reaction solution (1 cm^3) was added to a diethyl ether–water mixture (2 : 1 v/v, 3 cm^3). After the mixture had been stirred for 10 min, acetone in the ether phase was analyzed. The amount of acetone was determined from the ratio of the peak area of acetone to the peak area of toluene. In some experiments, another Xe lamp (LA-410UV, Hayashi Watch Works, Tokyo) was also used to evaluate the activity of H_2 formation under irradiation of visible light coming from a light source other than the above-mentioned Xe lamp.

2.4.2 Mineralization of acetic acid in aqueous suspensions of Au/TiO_2 under irradiation of visible light. Dried Au/TiO_2 powder (50 mg) was suspended in distilled water (5 cm^3) in a test tube. The aqueous mixture was bubbled with oxygen (O_2) and the test tube was sealed with a rubber septum. Acetic acid (50 μmol) was injected into the suspension and then irradiated with visible light from the 500 W Xe lamp (Ushio) with a Y-48 filter with magnetic stirring in a water bath continuously kept at 298 K. The amount of carbon dioxide (CO_2) in the gas phase of the reaction mixture was measured

using a gas chromatograph (GC-8A, Shimadzu) equipped with a Porapak QS column.

2.4.3 H_2 formation from ammonia in aqueous suspensions of Au/TiO_2 under irradiation of visible light. Dried photocatalyst powder (50 mg) was suspended in an aqueous solution (5 cm^3) containing ammonia (NH_3, 20 μmol) in a test tube, bubbled with Ar, and sealed with a rubber septum. The suspension was irradiated with visible light from the 500 W Xe lamp (Ushio) filtered with a Y-48 filter with magnetic stirring in a water bath continuously kept at 298 K. The amounts of H_2 and nitrogen (N_2) in the gas phase were measured using a Shimadzu GC-8A gas chromatograph equipped with an MS-5A column.

3. Results and discussion

3.1 Characterization of Au/TiO_2

Fig. 1 shows TEM photographs of Au(1.0 × 1)/TiO_2(723) and Au(0.25 × 4)/TiO_2(723). Small Au particles were observed in the TEM photograph of Au(1.0 × 1)/TiO_2(723) and the average diameter of Au particles was determined to be 1.2 nm, suggesting that the one-step photodeposition can be used to highly disperse Au nanoparticles on the surface of TiO_2. On the other hand, two types of Au particles having different sizes were observed in the TEM photographs of smaller and larger Au nanoparticles, although the number of larger particles was less than that of smaller particles. The average particle sizes of smaller and larger Au nanoparticles were determined to be 1.4 nm and 13 nm, respectively.

These results indicate that the Au sources added after the first photodeposition were deposited on Au particles previously formed on the TiO_2 surface, resulting in growth of the Au particles, and that the distribution of Au particles can be controlled by *Y*. The effect of *Y* on the distribution of Au nanoparticles of Au/TiO_2(723) samples having 1.0 wt% Au was examined in detail by changing *Y* from 1 to 10, and the results are shown in Fig. 2, in which *X* was simply determined by *Y* (*X* = 1.0/*Y*). The distribution of Au nanoparticles of Au/TiO_2(723) samples changed depending on *Y*, although the amount of Au loaded on TiO_2 was the same (1.0 wt%). The proportion of smaller Au particles (<5 nm) decreased with the increase in *Y*, while the proportion of larger Au particles (>10 nm) increased. Finally, smaller Au nanoparticles were not observed in Au(0.1 × 10)/TiO_2(723).

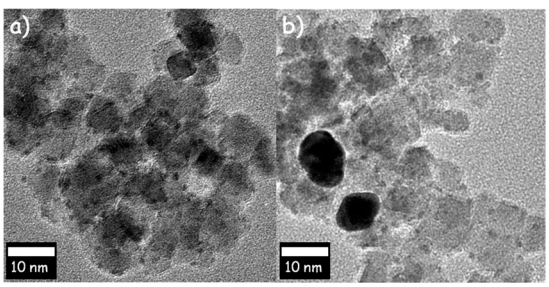

Fig. 1 TEM images of (a) Au(1.0 × 1)/TiO_2(723) and (b) Au(0.25 × 4)/TiO_2(723) samples.

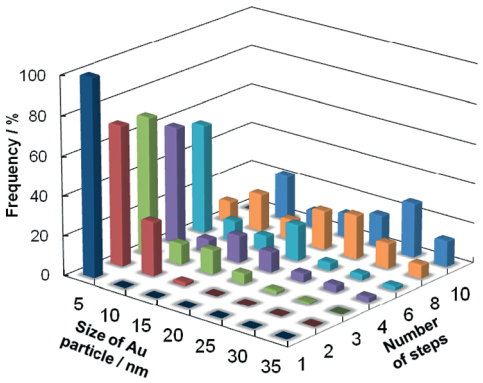

Fig. 2 Effect of the number of steps (*Y*) on the distribution of Au nanoparticles of Au(*X* × *Y*)/TiO_2(723) samples (*X* × *Y* = 1.0) prepared by the MS method.

Absorption spectra of Au(1.0 × 1)/TiO_2(723) and Au(0.25 × 4)/TiO_2(723) are shown in Fig. S1† (ref. 11*e*). Photoabsorption was observed at 550 nm, which was attributed to the SPR of the supported Au particles.[8–10] It should be noted that Au(0.25 × 4)/TiO_2(723) exhibited much stronger photoabsorption than Au(1.0 × 1)/TiO_2(723), although the amounts of Au loaded on TiO_2 were the same. Fig. 3(a) shows the intensities of photoabsorption at 550 nm of various Au/TiO_2(723) samples having 1.0 wt% Au. The intensity of photoabsorption of the samples increased with the increase in *Y* up to *Y* = 4 and tended to be saturated at *Y* > 4. This result suggests that the intensity of photoabsorption due to the SPR of Au was affected by the size of Au nanoparticles. Similar results have been obtained for plasmonic Au/TiO_2[11*e*] and Au/CeO_2[11*f*] photocatalysts and for unsupported Au nanoparticles.[13] In the last case, Shimizu *et al.*[13] reported that such observed features coincide with the prediction of the Mie theory.

3.2 Effect of the number of photodepositions on photocatalytic H_2 formation

Various 1.0 wt% Au/TiO_2(723) samples prepared by changing *Y* from 1 to 10 were used for formation of H_2 from 2-propanol in their aqueous suspensions under visible light

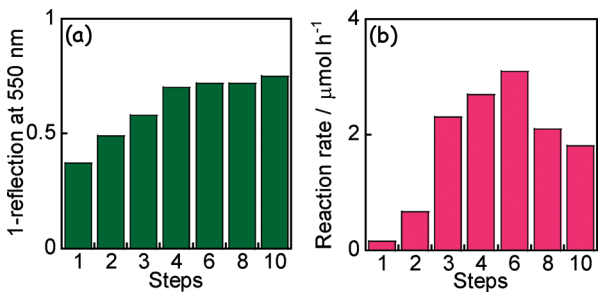

Fig. 3 Effect of the number of steps (*Y*) of Au(*X* × *Y*)/TiO_2(723) samples (*X* × *Y* = 1.0) on (a) "1-reflection" at 550 nm and (b) the rate of H_2 evolution from 2-propanol in aqueous suspensions under irradiation of visible light from a Xe lamp with a Y-48 filter.

irradiation from a Xe lamp with a Y-48 filter at 298 K. Just after irradiation of visible light, H_2 was evolved and the formation of H_2 continued almost linearly with irradiation time, indicating that the 1.0 wt% Au/TiO_2(723) samples were active for H_2 formation. The rates of H_2 evolution are shown in Fig. 3(b). The reaction rate increased until $Y = 6$ and the rates of H_2 evolution at $Y = 1$ and 6 were determined to be 0.15 and 3.1 μmol h^{-1}, respectively, *i.e.*, the Au(0.17 × 6)/TiO_2(723) sample exhibited a rate of H_2 evolution that was *ca.* 21 times higher than that of the Au(1.0 × 1)/TiO_2(723) sample even though the Au contents were the same. The intensity of SPR absorption seems to be one of the factors controlling the activity for H_2 production. However, the rates of H_2 evolution decreased at $Y = 8$ and 10 even though the light intensities of the samples were the same (Fig. 3(a)). Therefore, this tendency suggests that the presence of smaller Au nanoparticles as reduction sites was important as well as strong SPR absorption for H_2 evolution over Au/TiO_2(723) samples.

3.3 Effect of post-calcination

Post-calcination has been widely applied to control the particle size of Au loaded on various supports. Akita *et al.*[14] reported that the average size of small Au particles (~2 nm) in Au/TiO_2 increased with the increase in calcination temperature (>473 K) and that the small particles disappeared at temperature >573 K. When Au(0.25 × 4)/TiO_2(723) was calcined at 773 K in air, smaller Au particles having an average diameter of 1.4 nm disappeared (Fig. S2†), suggesting that these smaller particles merged with larger Au particles.[11e] Fig. 4 shows the effect of post-calcination temperature on the distribution of Au nanoparticles. It can be clearly seen that the proportion of smaller Au particles (<5 nm) decreased with the increase in post-calcination temperature and that Au particles on TiO_2 gradually grew with calcination. The effect of post-calcination temperature on photoabsorption of Au/TiO_2 samples at 550 nm is shown in Fig. 5(a).

Interestingly, calcination of the Au(0.25 × 4)/TiO_2(723) sample had almost no effect on the SPR, probably because further increase in the particle size had little effect on the SPR

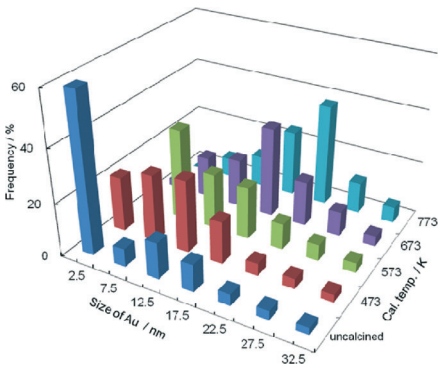

Fig. 4 Change in the distribution of Au particles by post-calcination of Au(0.25 × 4)/TiO_2(723).

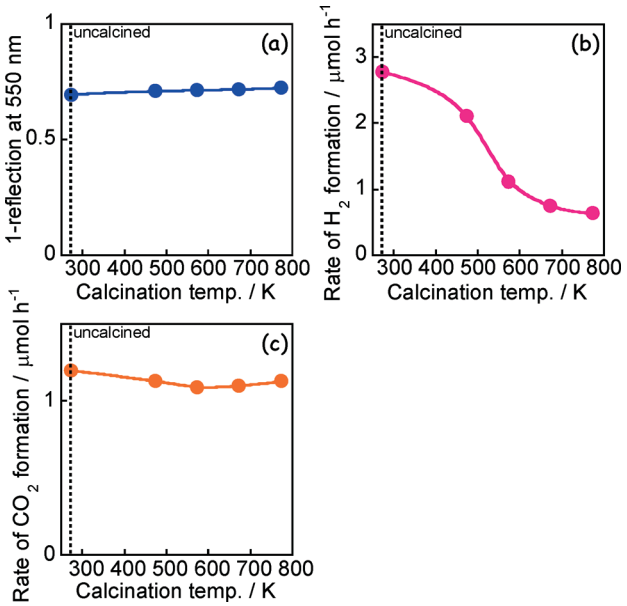

Fig. 5 Effects of post-calcination temperature on (a) "1-reflection" at 550 nm of Au(0.25 × 4)/TiO_2(723), (b) the rate of H_2 evolution from 2-propanol, and (c) the rate of CO_2 formation from acetic acid in the presence of O_2.

of the sample before calcination. Overall, post-calcination of the Au(0.25 × 4)/TiO_2(723) sample had an effect on smaller Au particles (<5 nm) but not on the SPR intensity. Therefore, the role of smaller Au particles (<5 nm) in H_2 evolution under irradiation of visible light was investigated by using Au(0.25 × 4)/TiO_2(723) and samples obtained by calcination of Au(0.25 × 4)/TiO_2(723) at various temperatures. Fig. 5(b) shows the effect of post-calcination temperature on the rate of H_2 evolution from 2-propanol in aqueous suspensions of these samples. The rate of H_2 formation decreased with the increase in post-calcination temperature, although the Au contents and SPR intensities of these samples were almost the same. These results suggest that smaller Au particles formed on TiO_2 by using the MS photodeposition method played important roles, such as in charge separation, electron storage and H^+ reduction but not in photoabsorption, in H_2 formation under irradiation of visible light.

Photocatalytic reaction in the presence of O_2, *i.e.*, photocatalytic mineralization, does not require a co-catalyst because O_2 is a good electron acceptor and one-electron reduction of O_2 by electrons in the conduction band of TiO_2 is possible without the aid of a co-catalyst. Therefore, Au(0.25 × 4)/TiO_2(723) and samples obtained by calcination of Au(0.25 × 4)/TiO_2(723) at various temperatures were used for mineralization of acetic acid in aqueous suspensions in the presence of O_2 under irradiation of visible light, and the effect of post-calcination on the rate of CO_2 formation is shown in Fig. 5(c). The rates of CO_2 formation were almost the same regardless of the temperature of post-calcination in contrast to the rates of H_2 formation (Fig. 5(b)). The different temperature dependency of CO_2 formation indicates that the smaller Au nanoparticles had little effect on the mineralization of acetic acid in the presence

of O_2. Two different dependencies support the idea that the smaller Au particles formed on TiO_2 work as a co-catalyst rather than as the main photocatalyst in H_2 evolution, *i.e.*, smaller Au particles have key roles in charge separation, electron storage and H^+ reduction rather than in photoabsorption, electron injection and substrate oxidation.

3.4 Effect of pre-calcination temperature

To examine the effects of physical properties and crystal structure, HyCOM-TiO_2 samples calcined at various temperatures (Z) [Z = 723–1273 K] were used as supports for Au particles. With the elevation in calcination temperature, S_{BET} of TiO_2 gradually decreased. Using the MS photodeposition method, 1.0 wt% Au particles were loaded on $TiO_2(Z)$, and Au(1.0 × 1)/$TiO_2(Z)$ and Au(0.25 × 4)/$TiO_2(Z)$ samples were prepared. These samples were used for H_2 evolution from 2-propanol under irradiation of visible light. Table 1 shows the yields of H_2 in the gas phase and acetone in the liquid phase after 10 h of irradiation as well as the specific surface areas of TiO_2, crystalline phases of TiO_2, intensities of photoabsorption at 550 nm due to SPR, and average sizes of smaller and larger Au particles. In the series of Au(1.0 × 1)/$TiO_2(Z)$ samples, only smaller Au particles were observed and the average size of the smaller Au particles increased with the elevation in calcination temperature. The increase in particle size can be explained by the decrease in S_{BET} of TiO_2 with calcination, *i.e.*, dispersion of Au on TiO_2 became worse with the decrease in S_{BET} of TiO_2. The intensity of photoabsorption due to SPR increased with the elevation in calcination temperature, although the Au contents were the same (1.0 wt%). These results indicate that photoabsorption due to SPR can be easily controlled by the calcination temperature of TiO_2 before Au photodeposition. In all of the Au(0.25 × 4)/$TiO_2(Z)$ samples, bimodal distributions of Au particles were observed. The average size of smaller Au particles increased with the decrease in S_{BET} of TiO_2, as in the case of Au(1.0 × 1)/$TiO_2(Z)$ samples, while the average sizes of larger Au particles were almost the same. Photoabsorption intensities at 550 nm of the Au(0.25 × 4)/$TiO_2(Z)$ samples were almost the same regardless of the calcination temperature and average size of the smaller Au particles in contrast to the Au(1.0 × 1)/$TiO_2(Z)$ samples. The behavior of the Au(0.25 × 4)/$TiO_2(Z)$ samples indicated that the photoabsorption of Au(0.25 × 4)/$TiO_2(Z)$ samples was determined by the larger Au particles in the range of 13–15 nm.

H_2 and acetone were formed in all anatase-type and anatase–rutile-mixed TiO_2 samples, whereas H_2 evolution from rutile-type TiO_2 samples was negligible. Since the conduction band of rutile-type TiO_2 is lower than that of anatase-type TiO_2, the position of the conduction band of the TiO_2 support seems to be important for Au/TiO_2 in H_2 evolution under the present reaction conditions. In the case of the Au(1.0 × 1)/$TiO_2(Z)$ samples, H_2 yield for 10 h reached a maximum (8.6 μmol) at Z = 1073 and further elevation in the calcination temperature led to a gradual decrease in the photocatalytic activity. The yield of H_2 seems to be determined complexly depending on the S_{BET}, crystal structure, particle size and photoabsorption due to SPR. On the other hand, the temperature dependency of the rate of Au(0.25 × 4)/$TiO_2(Z)$ samples was simple. The Au(0.25 × 4)/TiO_2(723) sample exhibited the largest H_2 yield (28 μmol) probably because the largest S_{BET} and the smallest average size of Au particles contributed to the adsorption of a large amount of 2-propanol and efficient H_2 evolution on the smaller Au particles, respectively. The ratios of the amount of H_2 formation to the amount of acetone over various Au(X × Y)/$TiO_2(Z)$ samples are also shown in Table 1. Values around unity were obtained in all samples except rutile-type TiO_2 (Z = 1273 K). Good agreement with yields of H_2 and acetone in these samples shows that the stoichiometric dehydrogenation of 2-propanol occurred as expressed in eqn (1):

$$(CH_3)_2CHOH \rightarrow (CH_3)_2CO + H_2 \quad (1)$$

As also clearly shown in Table 1, H_2 yields of the Au(0.25 × 4)/$TiO_2(Z)$ samples were 2–19 times higher than those of the Au(1.0 × 1)/$TiO_2(Z)$ samples. Since various factors intricately affect properties and functions of Au particles and final properties of Au/TiO_2, it is generally difficult to prepare an Au/TiO_2 sample satisfying all properties as a plasmonic photocatalyst by using a usual photodeposition method (Y = 1). The results of this study indicate that an Au/TiO_2

Table 1 Specific surface areas and crystal structures of various of TiO_2 samples and H_2 evolution from 2-propanol in aqueous suspensions of Au/TiO_2 under irradiation of visible light[a]

			Au(1.0 × 1)/$TiO_2(Z)$					Au(0.25 × 4)/$TiO_2(Z)$				
Z/K	S_{BET}[b] / $m^2\ g^{-1}$	Crystal structure[c]	D_{Au}[d] (smaller/larger)	1-R[e]	Y[f,h] (H_2)/ μmol	Y[g,h] (Ac)/ μmol	$Y(H_2)/Y(Ac)$	D_{Au}[d] (smaller/larger)	1-R[e]	Y[f,h] (H_2)/ μmol	Y[g,h] (Ac)/ μmol	$Y(H_2)/Y(Ac)$
723	97	A	1.2/—	0.39	1.5	1.5	1.0	1.4/13	0.70	28	29	0.97
823	91	A	1.4/—	0.40	2.3	2.4	0.96	1.5/13	0.70	27	26	1.0
973	54	A	2.5/—	0.42	4.1	4.2	0.98	2.8/14	0.71	24	23	1.0
1073	31	A	3.6/—	0.45	8.6	7.8	1.1	3.8/14	0.72	20	22	0.91
1173	13	A, R	4.2/—	0.48	2.4	2.3	1.0	4.5/14	0.73	5.6	5.7	0.98
1273	2.3	R	5.5/—	0.55	trace	trace	—	5.6/15	0.72	trace	trace	—

[a] TiO_2 was synthesized by the HyCOM method and calcined at Z (K) shown in parenthesis. [b] BET surface area. [c] A: anatase, R: rutile. [d] D_{Au}: average size of Au nanoparticles in Au/TiO_2. [e] Photoabsorption at 550 nm due to SPR. [f] H_2 yield for 10 h. [g] Acetone yield for 10 h. [h] 50 mg of photocatalyst and visible light in the range of 450–600 nm (83 mW cm^{-2}).

sample with excellent properties as a plasmonic photocatalyst can be easily prepared by using the MS photodeposition method.

3.5 Effect of cut-off filters

Fig. 6 shows the effect of cut-off filters set in the Xe lamp on H_2 evolution from 2-propanol in aqueous suspensions of Au(0.25 × 4)/TiO_2(723). Fig. 6 is different from an ordinary action spectrum, and the results indicate both the effects of the wavelength of light and the amount of photons. The rate of H_2 formation decreased with the increase in the filter number, corresponding to the decrease in photoabsorption. Specifically, a large decrease in the rate was observed when the O58 cut-off filter was used. In the case of Au/cerium(IV) oxide, photoabsorption in the range of 600–700 nm mainly due to light scattering scarcely contributed to the photocatalytic reaction.[11c] Similarly, the large decrease in the rate observed in the Au(0.25 × 4)/TiO_2(723) sample is explained by the same reason.

3.6 Effect of light intensity

Au(1.0 × 1)/TiO_2(723) and Au(0.25 × 4)/TiO_2(723) samples were used for H_2 formation from 2-propanol in aqueous suspensions under irradiation by light from a Xe lamp with a Y-44 filter with various light intensities (3.2–46 mW cm^{-2}) as shown in Fig. 7(a). Fig. 7(b) shows the effect of light intensity on the rate of H_2 formation. The rates increased with the increase in light intensity in both samples, and the rates of Au(0.25 × 4)/TiO_2(723) were always higher than those of Au(1.0 × 1)/TiO_2(723). We noted that the light intensity had different effects on the rate of H_2 formation over the two samples. The ratio of the rates of H_2 formation over the two samples (R4/R1) is shown in Fig. 7(c). The values of R4/R1 decreased with the increase in light intensity, which was due to the decrease in efficiency of Au(0.25 × 4)/TiO_2(723) (Fig. 7(b)). The decrease in efficiency of photocatalytic reactions under irradiation of intense light is often observed in semiconductor photocatalysts and is generally explained by increased electron–hole recombination probability. Similarly, the decrease in the rates of Au(0.25 × 4)/TiO_2(723) under irradiation of intense light is explained by the same reason. In other words, the efficiency of Au(0.25 × 4)/TiO_2(723) is more pronounced under irradiation of weaker light.

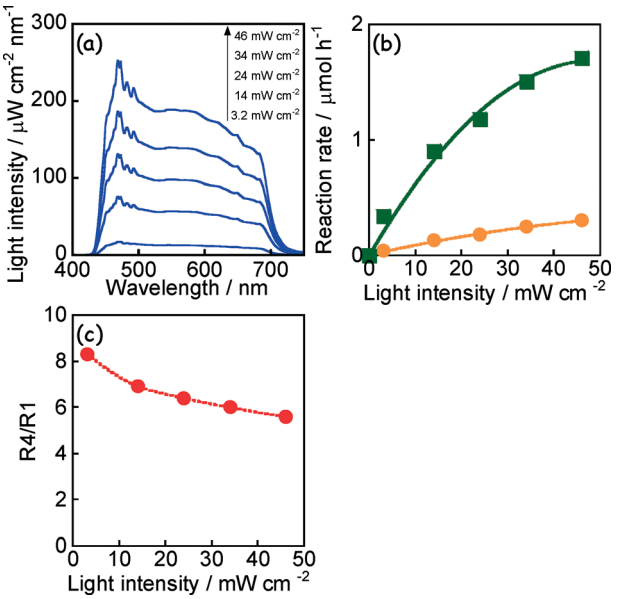

Fig. 7 (a) Intensity of visible light irradiated to reaction systems from a Xe lamp with a Y-44 cut-off filter and effect of light intensity on (b) the rate of H_2 formation from 2-propanol in aqueous suspensions of Au(1.0 × 1)/TiO_2(723) (circles) and Au(0.25 × 4)/TiO_2(723) (squares) and (c) the ratio of the rates.

3.7 H_2 formation from NH_3

To extend the possibility of Au/TiO_2 for H_2 formation under visible light, NH_3 as biomass waste in water was used as a substrate. Fig. 8 shows time courses of the evolution of H_2 and N_2 from NH_3 in an aqueous suspension of Au(0.25 × 4)/TiO_2(723) under irradiation of visible light. Since H_2 and N_2 increased linearly with photoirradiation time, the rates of H_2 and N_2 evolution were determined to be 0.84 and

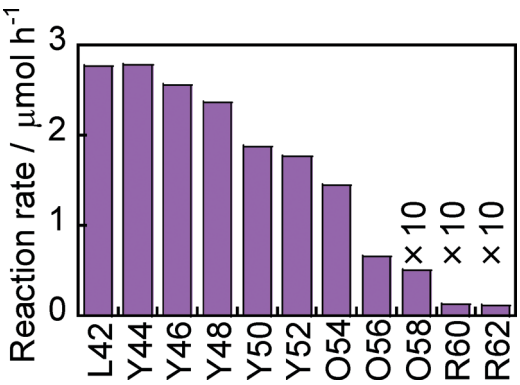

Fig. 6 Effect of cut-off filter sets in the Xe lamp on H_2 evolution from 2-propanol in aqueous suspensions of Au(0.25 × 4)/TiO_2(723).

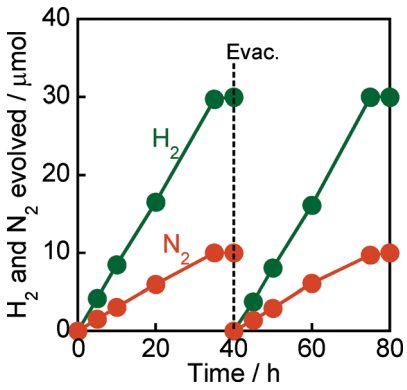

Fig. 8 Time courses of evolution of H_2 and N_2 from NH_3 in an aqueous suspension of Au(0.25 × 4)/TiO_2(723) under irradiation of visible light from a Xe lamp with a Y-48 filter. After 40 h of irradiation and evacuation, additional NH_3 (20 μmol) was injected and the suspension was irradiated again.

0.29 μmol h^{-1}, respectively. After photoirradiation for 35 h, H_2 and N_2 evolution was almost saturated at around 30 and 10 μmol (H_2/N_2 ratio of 3.0), which corresponded to the initial amount of NH_3 (20 μmol), indicating that NH_3 was almost completely decomposed to H_2 and N_2 (eqn (2)) over Au(0.25 × 4)/TiO_2(723) under irradiation of visible light.

$$2NH_3 \rightarrow N_2 + 3H_2 \quad (2)$$

To evaluate the stability of Au/TiO_2 in H_2 and N_2 production from NH_3, Au(0.25 × 4)/TiO_2(723) was used again. Irradiation of the reaction mixtures under visible light again induced evolution of H_2 and N_2, and the formation continued from 40 h to 80 h without deactivation.

Conclusions

Gold (Au)-loaded titanium(IV) oxide (Au/TiO_2) having both smaller and larger Au particles was successfully prepared by the multi-step (MS) photodeposition method. The Au particle distribution and photoabsorption properties of Au/TiO_2 can be controlled by conditions of the MS photodeposition, post-calcination of Au/TiO_2 and properties of TiO_2 before Au loading. In hydrogen (H_2) formation from 2-propanol in aqueous suspensions of Au/TiO_2 under irradiation of visible light, the co-existence of large (>10 nm) and small (<5 nm) Au particles was indispensable for higher activities, which contributed to strong photoabsorption due to surface plasmon resonance (SPR) and efficient H_2 evolution (proton reduction), respectively. Au/TiO_2 having a bimodal Au distribution can be applied for the stoichiometric decomposition of ammonia to H_2 and nitrogen under visible light irradiation. On the other hand, in the case of mineralization of acetic acid in the presence of oxygen (O_2), small Au particles are not requisite because O_2 is a good electron acceptor and one-electron reduction of O_2 by electrons in the conduction band of TiO_2 is possible without the aid of a co-catalyst. These results suggest that separate loading of co-catalyst particles without alloying with Au particles is effective for enhancing the activities of an Au plasmonic photocatalyst in reactions in which reaction rates are controlled by electron consumption.

Acknowledgements

This work was partly supported by a Grant-in-Aid for Scientific Research (no. 23560935) from the Ministry of Education, Culture, Sports, Science, and Technology (MEXT) of Japan. The authors (H. K. and A. T.) are grateful for financial support from the Iketani Science and Technology Foundation. One of the authors (A. T.) appreciates the Japan Society for the Promotion of Science (JSPS) for the Research Fellowship for Young Scientists.

Notes and references

1 (*a*) M. A. Fox and M. T. Dulay, *Chem. Rev.*, 1993, **93**, 341; (*b*) M. R. Hoffmann, S. T. Martin, W. Choi and D. W. Bahnemann, *Chem. Rev.*, 1995, **95**, 69.

2 (*a*) F. Mahdavi, T. C. Bruton and Y. Li, *J. Org. Chem.*, 1993, **58**, 744; (*b*) J. L. Ferry and W. H. Glaze, *Langmuir*, 1998, **14**, 3551; (*c*) K. Imamura, K. Hashimoto and H. Kominami, *Chem. Commun.*, 2012, **48**, 4356; (*d*) H. Tada, T. Ishida, A. Takao and S. Ito, *Langmuir*, 2004, **20**, 7898; (*e*) Y. Shiraishi, Y. Togawa, D. Tsukamoto, S. Tanaka and T. Hirai, *ACS Catal.*, 2012, **2**, 2475–2481; (*f*) K. Fuku, K. Hashimoto and H. Kominami, *Chem. Commun.*, 2010, **46**, 5118; (*g*) K. Fuku, K. Hashimoto and H. Kominami, *Catal. Sci. Technol.*, 2011, **1**, 586.

3 (*a*) T. Kawai and T. Sakata, *Nature*, 1980, **286**, 474; (*b*) K. Shimura and H. Yoshida, *Energy Environ. Sci.*, 2011, **4**, 2467; (*c*) H. Kominami, H. Nishimune, Y. Ohta, Y. Arakawa and T. Inaba, *Appl. Catal., B*, 2012, **111–112**, 297; (*d*) H. Yuzawa, T. Mori, H. Itoh and H. Yoshida, *J. Phys. Chem. C*, 2012, **116**, 4126.

4 R. Asahi, T. Morikawa, T. Ohwaki, K. Aoki and Y. Taga, *Science*, 2001, **293**, 269.

5 T. Ohno, M. Akiyoshi, T. Umebayashi, K. Asai, T. Mitui and M. Matsumura, *Appl. Catal., A*, 2004, **265**, 115.

6 H. Irie, S. Miura, K. Kamiya and K. Hashimoto, *Chem. Phys. Lett.*, 2008, **457**, 202.

7 (*a*) H. Kisch, L. Zang, C. Lange, W. F. Maier, C. Antonius and D. Meissner, *Angew. Chem., Int. Ed.*, 1998, **37**, 3034; (*b*) H. Kominami, K. Sumida, K. Yamamoto, N. Kondo, K. Hashimoto and Y. Kera, *Res. Chem. Intermed.*, 2008, **34**, 587; (*c*) S. Kitano, K. Hashimoto and H. Kominami, *Appl. Catal., B*, 2011, **101**, 206; (*d*) S. Kitano, N. Murakami, T. Ohno, Y. Mitani, Y. Nosaka, H. Asakura, K. Teramura, T. Tanaka, H. Tada, K. Hashimoto and H. Kominami, *J. Phys. Chem. C*, 2013, **117**, 11008.

8 (*a*) X. Chen, S. Shen, L. Guo and S. S. Mao, *Chem. Rev.*, 2010, **110**, 6503; (*b*) R. M. Navarro, M. C. Sánchez-Sánchez, M. C. Alvarez-Galvan, F. del Valle and J. L. G. Fierro, *Energy Environ. Sci.*, 2009, **2**, 35.

9 (*a*) M. Xiao, R. Jiang, F. Wang, C. Fang, J. Wang and J. C. Yu, *J. Mater. Chem. A*, 2013, **1**, 5790; (*b*) S. C. Warren and E. Thimsen, *Energy Environ. Sci.*, 2012, **5**, 5133; (*c*) X. Zhou, G. Liu, J. Yu and W. Fan, *J. Mater. Chem.*, 2012, **22**, 21337; (*d*) S. Linic, P. Christopher and D. B. Ingram, *Nat. Mater.*, 2011, **10**, 911.

10 (*a*) Y. Tian and T. Tatsuma, *J. Am. Chem. Soc.*, 2005, **127**, 7632; (*b*) A. Furube, L. Du, K. Hara, R. Katoh and M. Tachiya, *J. Am. Chem. Soc.*, 2007, **129**, 14852; (*c*) S. Naya, M. Teranishi, T. Isobe and H. Tada, *Chem. Commun.*, 2010, **46**, 815; (*d*) E. Kowalska, R. Abe and B. Ohtani, *Chem. Commun.*, 2009, 241; (*e*) E. Kowalska, O. O. P. Mahaney, R. Abe and B. Ohtani, *Phys. Chem. Chem. Phys.*, 2010, **12**, 2344; (*f*) C. G. Silva, R. Juarez, T. Marino, R. Molinari and H. Garcia, *J. Am. Chem. Soc.*, 2011, **133**, 595; (*g*) H. Yuzawa, T. Yoshida and H. Yoshida, *Appl. Catal., B*, 2012, **115**, 294; (*h*) X. Ke, X. Zhang, J. Zhao, S. Sarina, J. Barry and H. Zhu, *Green Chem.*, 2013, **15**, 236.

11 (*a*) H. Kominami, A. Tanaka and K. Hashimoto, *Chem. Commun.*, 2010, **46**, 1287; (*b*) H. Kominami, A. Tanaka and K. Hashimoto, *Appl. Catal., A*, 2011, **397**, 121; (*c*) A. Tanaka, K. Hashimoto and H. Kominami, *ChemCatChem*, 2011, **3**,

1619; (*d*) A. Tanaka, K. Hashimoto and H. Kominami, *Chem. Commun.*, 2011, **47**, 10446; (*e*) A. Tanaka, S. Sakaguchi, K. Hashimoto and H. Kominami, *Catal. Sci. Technol.*, 2012, **2**, 907; (*f*) A. Tanaka, K. Hashimoto and H. Kominami, *J. Am. Chem. Soc.*, 2012, **134**, 14526; (*g*) A. Tanaka, A. Ogino, M. Iwaki, K. Hashimoto, A. Ohnuma, F. Amano, B. Ohtani and H. Kominami, *Langmuir*, 2012, **28**, 13105; (*h*) A. Tanaka, S. Sakaguchi, K. Hashimoto and H. Kominami, *ACS Catal.*, 2013, **3**, 79; (*i*) A. Tanaka, K. Hashimoto, B. Ohtani and H. Kominami, *Chem. Commun.*, 2013, **49**, 3419–3421; (*j*) A. Tanaka, Y. Nishino, S. Sakaguchi, T. Yoshikawa, K. Imamura, K. Hashimoto and H. Kominami, *Chem. Commun.*, 2013, **49**, 2551; (*k*) A. Tanaka, K. Nakanishi, R. Hamada, K. Hashimoto and H. Kominami, *ACS Catal.*, 2013, **3**, 1886.

12 (*a*) H. Kominami, M. Kohno, Y. Takada, M. Inoue, T. Inui and Y. Kera, *Ind. Eng. Chem. Res.*, 1999, **38**, 3925; (*b*) H. Kominami, S.-Y. Murakami, J.-I. Kato, Y Kera and B Ohtani, *J. Phys. Chem. B*, 2002, **106**, 10501.

13 T. Shimizu, T. Teranishi, S. Hasegawa and M. Miyake, *J. Phys. Chem. B*, 2003, **107**, 2719.

14 T. Akita, P. Lu, S. Ichikawa, K. Tanaka and M. Haruta, *Surf. Interface Anal.*, 2001, **31**, 73.

